Functionalization and Hydrogenation of Carbon Chains Derived from CO

Maria Batuecas, Richard Y. Kong, Andrew J. P. White, Mark, R. Crimmin*

Department of Chemistry, MSRH, Imperial College London, 82 Wood Lane, Shepherds Bush, London, W12 0BZ, UK.

ABSTRACT: Selective reactions that combine H_2, CO and organic electrophiles (aldehyde, ketones, isocyanide) to form hydrogenated C_3 and C_4 carbon chains are reported. These reactions proceed by CO homologation mediated by $[W(CO)_6]$ and an aluminum(I) reductant, followed by functionalization and hydrogenation of the chain ends. A combination of kinetics (rates, KIEs) and DFT calculations has been used to gain insight into a key step which involves hydrogenation of a metallocarbene intermediate. These findings expand the extremely small scope of systems that combine H_2 and CO to make well-defined products with complete control over chain length and functionality.

The controlled polymerization, hydrogenation and dehydration of CO/H_2 mixtures to form hydrocarbons by the Fischer-Tropsch (F-T) process is an essential reaction for industry.[1,2] There has long been interest in controlling the selectivity of this reaction.[3] Many have advocated the potential of homogeneous catalysts to lead to reaction products with defined molecular weight and oxygen content.[4,5]

Despite these ambitions, homogeneous reactions that lead to F-T products are incredibly rare.[4,6–10] Our fundamental understanding of this type of reactivity is limited; there are only a handful of well-defined systems that combine CO and H_2 in a single reaction sequence to form either hydrocarbon (C_xH_y) or oxygenate ($C_xH_yO_z$) products. In 1991, Lippard and co-workers reported the reductive coupling and hydrogenation of CO to form *cis*-disiloxyethylene compounds, mediated by vanadium complexes.[11] More recently, Peters and Suess reported a similar product from the hydrogenation of a CO derived iron dicarbyne.[12] Hou and co-workers have documented the hydrodeoxygenative cyclotetramerization of CO by a trinuclear titanium poly(hydride) complex to form a cyclobutanone product.[13] Stephan and co-workers have shown that a simple lithium amide base ($LiNCy_2$) can react with CO/H_2 mixtures to form small amounts (<10 % yield) of an a-hydroxy amide derived from coupling and hydrogenation of two CO units.[14]

These systems represent the limit of knowledge in this field and have clear limitations. To date only C_2 and C_4 hydrogenated chain-growth products have been isolated. There are no examples of generating more complex products by incorporating organic electrophiles (other than CO) within the carbon chain. There is also a lack of detailed mechanistic information on the hydrogenation step. A broader scope and deeper understanding of these types of transformations could be an important factor in ultimately achieving selective F-T catalysis.

In this paper, we describe the direct hydrogenation of a series of CO homologation products, including for the first time, well-defined reactivity of C_3 carbon chains. We show that F-T products can be obtained by reaction with CO, organic electrophiles, a main group reductant and H_2. We provide a mechanistic description of the key hydrogenation step, shedding light on a key C–H bond formation pathway of relevance to F-T catalysis.

We have previously reported carbon-chain growth reactions from **1**, $[W(CO)_6]$ and CO.[15,16] Reaction of **2** with benzophenone at 100 °C in C_6D_6 led to the formation of **3a** and **4a** in 81 % yield, in a 4:1 ratio based on ^{1}H NMR spectroscopy (Scheme 1).

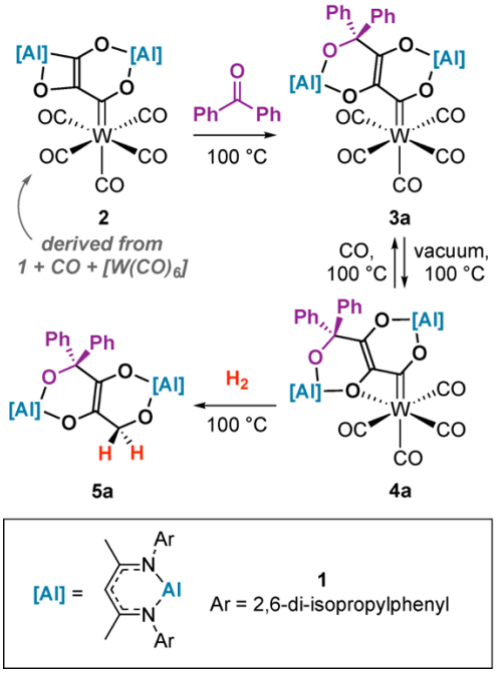

Scheme 1. Reactions of **2** with benzophenone and H_2.

The conversion of **3a** to **4a** is reversible. Heating mixtures of **3a**+**4a** under 1 atm. of CO for 12 h at 100 °C led to complete conversion to **3a**. Upon heating under vacuum, **3a** partially converts back to **4a**. DFT calculations are consistent with the reversible reaction. Formation of **4a** from **3a** was calculated to be endergonic ($\Delta G°_{298K}$ = +6.2 kcal mol^{-1}) and occur *via* an interchange mechanism ($\Delta G^{‡}_{298K}$ = +25.4 kcal mol^{-1}) (Figure 1a).

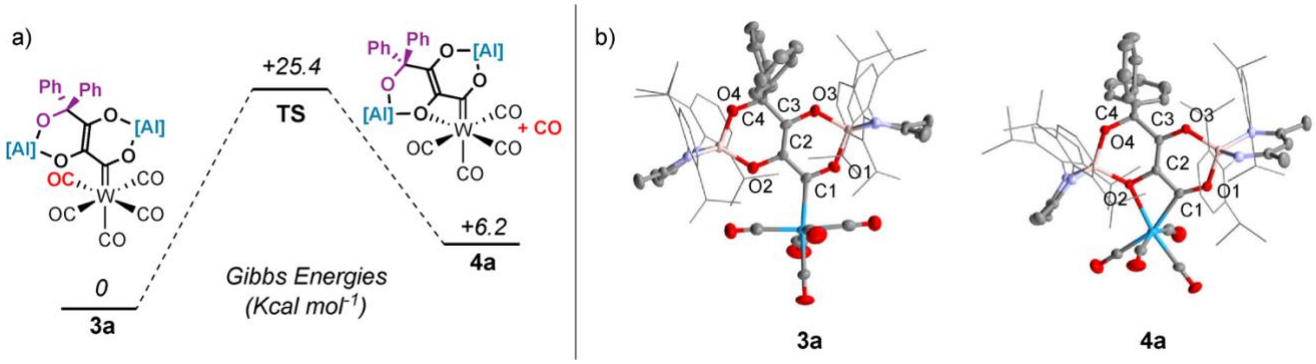

Figure 1: a). DFT calculated mechanism for transformation of **3a** to **4a**. b). Solid state structures of **3a** and **4a**.

Compounds **3a** and **4a** have been characterized by multinuclear NMR and IR spectroscopy. In C_6D_6 solution, **3a** and **4a** display ^{13}C NMR resonances for the metallocarbene ligand at δ = 315.6 and 310.9 ppm respectively. The equatorial and axial carbonyl ligands of **3a** are magnetically inequivalent and appear at d = 203.3 and 205.1 ppm. For comparison, **4a** shows three resonances for the CO ligands in the ^{13}C NMR spectrum at δ = 215.5, 218.8 and 221.4 ppm due to the reduction in symmetry. IR spectroscopy is consistent with a change in geometry around the metal center from **3a** (ν(CO) = 2050, 1897 and 1871 cm^{-1}) to **4a** (ν(CO) = 1988, 1874, 1862 and 1825 cm^{-1}) due to CO dissociation.

In the solid-state, the W–C bond length of **3a** of 2.269(4) Å is longer than that of 2.195(3) Å found in **2**. Formation of the k^2-C,O coordination mode occurs with a large distortion away from an ideal octahedral geometry at W, an effect driven by the acute bite angle of 60.9(1) ° of the chelating ligand.[17] This distortion also influences the geometry at the metallocarbene fragment. The W–C^1–O^1 and W–C^1–C^2 angles in **3a** are 115.4(2) and 130.0(3) °, close to the expected value for a sp^2-hybridised carbon center. Upon chelation to form **4a** these values become increasingly distorted away from an ideal geometry with the W–C^1–O^1 angle expanding to 141.3(2) ° and W–C^1–C^2 angle contracting to 99.4(2) °.

Complex **4a** reacts with H_2. Treatment of a benzene solution of **4a** with H_2 (1 atm.) at 100 ºC for 2 h led to the corresponding F-T type product **5a** in >95% NMR yield (Scheme 1). Attempts to crystallise this complex were unsuccessful, however compound **5a** was characterised by diagnostic resonances at δ = 4.38 ppm and δ = 67.9 ppm, in the ^{1}H and ^{13}C NMR spectra respectively, assigned to the new methylene group formed upon H_2 addition. Further analysis of the reaction mixtures revealed $[W(CO)_6]$ and $[W(CO)_3(\eta^6\text{-}C_6D_6)]$ as side products of hydrogenation. An isotope labelling experiment in which **4a** was reacted with D_2 provided clear evidence for the formation of **5a**-D_2 with the methylene group resonating at d = 4.38 ppm in the ^{2}H NMR spectrum. Hydrogenation of **3a** also directly leads to **5a**,[18] as does the reaction of **2**, H_2 and benzophenone at 100 °C.

The reaction scope was developed further (Table 1). A series of C_4 homologation complexes (**3b-e**) were prepared from the reaction of **2** with CO,[15] 3-methylbenzaldehyde, 2-butanone, and 2,6-dimethylphenyl isocyanide. These reactions proceeded smoothly in all cases demonstrating that $C_3 \rightarrow C_4$ chain growth is possible with a range of electrophiles. Hydrogenation of **3b-e** led to **5b-e** in 60-95 % NMR yield. In the case of **3e**, the expected hydrogenation product can be observed spectroscopically but isomerizes to a more stable enamine tautomer under the reaction conditions. The reaction is not limited to C_4 homologation products, as direct hydrogenation of **2** was also possible leading to the formation of the C_3 analogue **5f**. Remarkably, **5b** could also be obtained in 50 % NMR yield from a direct reaction of $[W(CO)_6]$, **1** and syngas (1:1 mixture of H_2/CO, 1 atm.) after 10 days at 100 °C. While the reaction is slow, this experiment shows that there is an element of self-organisation in this system as F-T type products to be formed in a single step from simple starting materials.

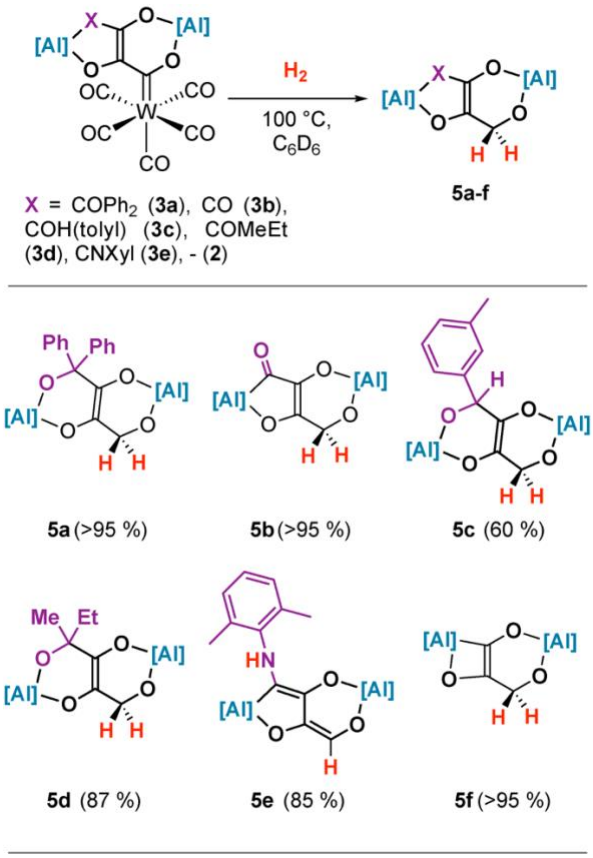

Table 1. Scope of hydrogenation reaction. Yield determined by ^{1}H NMR spectroscopy using 1,3,5-trimethoxybenzene as external standard.

Further experiments and calculations were undertaken to gain insight into the key hydrogenation step. The reaction of **3a** with H_2 (1 atm.) in benzene-d_6 at 100 ºC was monitored as a function of time by *in situ* ^{1}H NMR spectroscopy. Kinetic data show that hydrogenation of **3a** occurs as consecutive reactions with **4a** as intermediate (supporting information, Figure S6). Hydrogenation of **4a** was also monitored by ^{1}H NMR spectroscopy. Kinetic data could be fitted to pseudo-1st order decay of [**4a**]. The rate constant for the H_2 reaction was found to be $k_{obs}(H_2)$ = 6.28 (±0.06) x 10^{-4} s^{-1} (Figure 2). Side-by-side kinetic runs with H_2 and D_2 gave a KIE of 1.02 (±0.01).

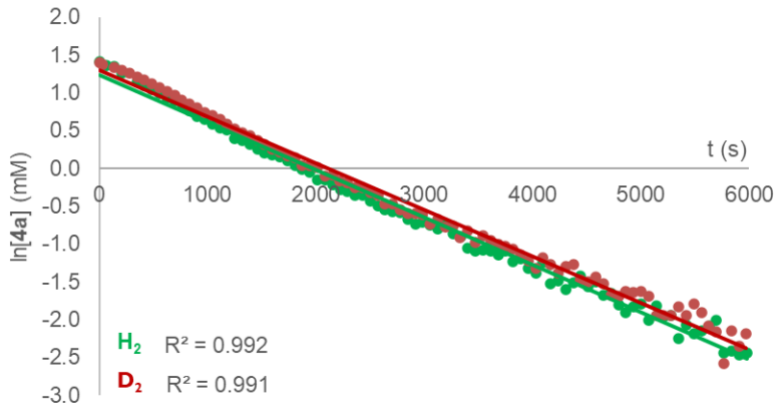

Figure 2. Ln[**4a**] versus time plot for reaction of **4a** with H_2 (green) and D_2 (red); $[\mathbf{4a}]_0$ = 4.6 mM.

A series of plausible pathways for the hydrogenation reaction were calculated by DFT. The lowest energy pathway is depicted in Figure 3. The calculated mechanism is initiated by η^2-dihydrogen coordination to complex **4a** to give **Int-1**.[19–23] Formation of this intermediate occurs *via* an interchange mechanism ($\Delta G^{\ddagger}_{298K}$ = +21.7 kcal mol^{-1}). Oxidative addition of H_2 to the W centre from **Int-1** gives the dihydride intermediate **Int-2** *via* a low energy barrier transition state **TS-2** followed by a barrierless migration of one of the hydrides to the carbon atom of the metallocarbene to give **Int-3**. There is precedent for this type of 1,2-migration involving hydride and metallocarbene ligands.[24–26] Prior calculations are consistent with a low energy process.[27–29] **Int-3** is stabilised by an agostic interaction of the newly formed C–H bond to W.[30] After two consecutive rotations steps via **TS-4** and **TS-5**, **Int-3** leads to **Int-5** which is stabilised by coordination of an oxygen atom of the carbon chain. **Int-5** dissociates a CO ligand through **TS-6** to give **Int-6**. **Int-6** then rotates again through **Int-7** to **Int-8** which is preorganised for reductive elimination *via* **TS-9** to afford the thermodynamically stabilised **Int-9**, a precursor of the final products.[31] The barrier for the reductive elimination step is low ($\Delta G^{\ddagger}_{298K}$ = +11.7 kcal mol^{-1}).

Overall, this calculated mechanism proceeds via a series of established fundamental steps of organometallic compounds namely: (i) ligand substitution (ii) oxidative addition, (iii) migratory insertion, and (iv) reductive elimination. The Gibbs activation energy corresponds to energy span from **4a** to **TS-5** ($\Delta G^{\ddagger}_{298K}$ = +34.8 kcal mol^{-1}).[32] The rate-limiting sequence involves coordination of H_2, oxidative addition of H_2, hydride migration from W to C and CO dissociation. The predicted pathway is consistent across a series of DFT functionals.

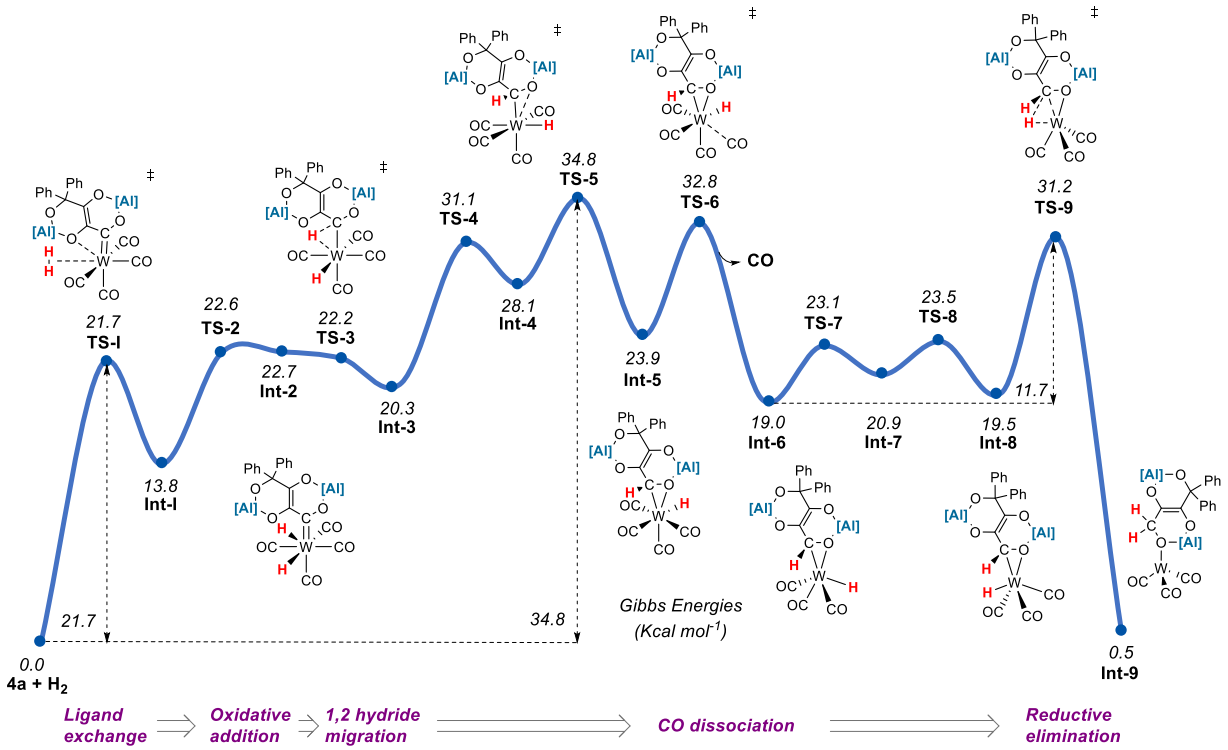

Figure 3. DFT calculated mechanism for hydrogenation of **4a**.

Consideration of the calculated reaction mechanism suggests that the assignment of a KIE in this system is complex. Although the experimentally determined KIE of 1.02 (±0.01) could be interpreted as a simple step not involving hydrogen atoms, based on the calculations it more likely arises from the combination of individual KIEs (or EIEs) from a series of steps. While oxidative addition of H_2 to W is expected to show a normal primary KIE, H_2 binding often occurs with an inverse IE.[33] Similarly, based on the stretching vibrational modes, hydride migration from W to C might be expected to occur with an inverse KIE.[34]

In summary, we report the formation of F-T type products from the combination of H_2, CO, organic electrophiles, and a main group reductant. The reaction scope allows the generation of both C_3 and C_4 chains with complete selectively. The hydrogenation step is mediated by the transition metal which likely plays a key role through activation of H_2 at a site adjacent to a metallocarbene ligand. These findings greatly expand the scope and understanding of reactivity for homogeneous systems reported that combine H_2 and CO to make hydrogenated carbon-chains.

ASSOCIATED CONTENT

X-ray data are deposited in the Cambridge Crystallographic database: CCDC 2130349-2130351 and 2129490-2129492. Primary data (.mnova, .txt and .xyz) are available from Imperial's Research Data Repository and available through the following link: 10.14469/hpc/10042

AUTHOR INFORMATION

Corresponding Author

*m.crimmin@imperial.ac.uk

Author Contributions

The manuscript was written through contributions of all authors. All authors have given approval to the final version of the manuscript.

ACKNOWLEDGMENT

We thank Imperial College London for the award of a President's Scholarship (RYK). We also thank the EPSRC for project funding (EP/S036628/1).

REFERENCES

(1) Schulz, H. Short History and Present Trends of Fischer-Tropsch Synthesis. *Appl. Catal. A Gen.* **1999**, *186* (1–2), 3–12.

(2) De Klerk, A. Fischer–Tropsch Process 1. *Kirk-Othmer Encyclopedia of Chemical Technology*; John-Wiley and Sons, Inc.: Hoboken, NJ, 2013; pp 1–36.

(3) Anderson, R. B.; Friedel, R. A.; Storch, H. H. Fischer-Tropsch Reaction Mechanism Involving Stepwise Growth of Carbon Chain. *J. Chem. Phys.* **1951**, *19* (3), 313–319.

(4) West, N. M.; Miller, A. J. M.; Labinger, J. A.; Bercaw, J. E. Homogeneous Syngas Conversion. *Coord. Chem. Rev.* **2011**, *255* (7–8), 881–898.

(5) Kong, R. Y.; Crimmin, M. R. Cooperative Strategies for CO Homologation. *Dalt. Trans.* **2020**, *49* (46), 16587–16597.

(6) B, D. Homogeneous Catalytic Hydrogenation of Carbon Monoxide: Ethylene Glycol and Ethanol from Synthesis Gas. *Adv. Catal.* **1983**, *32* (C), 325–416.

(7) Labinger, J. A. Approaches to Homogeneously Catalyzed CO Hydrogenation: A Personal Retrospective. *J. Organomet. Chem.* **2017**, *847*, 4–12.

(8) Maitlis, P. M. Fischer-Tropsch, Organometallics, and Other Friends. *J. Organomet. Chem.* **2004**, *689* (24 SPEC. ISS.), 4366–4374.

(9) Qi, Z.; Chen, L.; Zhang, S.; Su, J.; Somorjai, G. A. Integrating the Fields of Catalysis: Active Site Engineering in Metal Cluster, Metal Organic Framework and Metal Single Site. *Top. Catal.* **2020**, *63* (7–8), 628–634.

(10) Demitras, G. C.; Muetterties, E. L. Metal Clusters in Catalysis. 10. A New Fischer-Tropsch Synthesis. *J. Am. Chem. Soc.* **1977**, *99* (8), 2796–2797.

(11) Protasiewicz, J. D.; Lippard, S. J. Vanadium-Promoted Reductive Coupling of CO and Facile Hydrogenation To Form Cis-Disiloxyethylenes. *J. Am. Chem. Soc.* **1991**, *113* (17), 6564–6570.

(12) Suess, D. L. M.; Peters, J. C. A CO-Derived Iron Dicarbyne That Releases Olefin upon Hydrogenation. *J. Am. Chem. Soc.* **2013**, *135* (34), 12580–12583.

(13) Hu, S.; Shima, T.; Hou, Z. Hydrodeoxygenative Cyclotetramerization of Carbon Monoxide by a Trinuclear Titanium Polyhydride Complex. *J. Am. Chem. Soc.* **2020**, *142* (47), 19889–19894.

(14) Xu, M.; Qu, Z. W.; Grimme, S.; Stephan, D. W. Lithium Dicyclohexylamide in Transition-Metal-Free Fischer-Tropsch Chemistry. *J. Am. Chem. Soc.* **2021**, *143* (2), 634–638.

(15) Kong, R. Y.; Crimmin, M. R. Carbon Chain Growth by Sequential Reactions of CO and CO_2 with [$W(CO)_6$] and an Aluminum(I) Reductant. *J. Am. Chem. Soc.* **2018**, *140* (42), 13614–13617.

(16) Kong, R. Y.; Batuecas, M.; Crimmin, M. R. Reactions of aluminium(I) with transition metal carbonyls: scope, mechanism and selectivity of CO homologation. *Chem. Sci.* **2021**, *12*, 14845-14854.

(17) Hart, I. J.; Jeffery, J. C.; Lowry, R. M.; Stone, F. G. A. Acyl–Alkylidyne Coupling in the Synthesis

of Dinuclear Complexes. *Angew. Chem. Int. Ed.* **1988**, *27* (12), 1703–1705.

(18) To check if insertion could occur also into hydrogenated products, reaction of **3a** with benzophenone was tested and no reactivity was observed, suggesting that the reaction follows the sequence insertion-hydrogenation.

(19) Although different geometries for **Int-1** can be proposed, rotational barriers for H_2 ligand have been calculated to be low in energy for this molecule ($\Delta G°_{298K}$ = +3.2-6.8 kcal mol^{-1} and $\Delta G^{‡}_{298K}$ = +0.7-4.5 kcal mol^{-1}) and are in agreement with previous results for related molecules (see supporting information).

(20) Hay, P. J. Ab Initio Theoretical Studies of Dihydrogen Coordination vs Oxidative Addition of H_2 to Five-Coordinate Tungsten Complexes. *J. Am. Chem. Soc.* **1987**, *109* (3), 705–710.

(21) Hay, P. J. Ab Initio Theoretical Studies of a Novel Tungsten Dihydrogen Complex. *Chem. Phys. Lett.* **1984**, *103* (January), 466–469.

(22) Juergen Eckert, Gregory J. Kubas, John H. Hall, P. Jeffrey Hay, and C. M. B. Molecular Hydrogen Complexes. 6. The Barrier to Rotation of η^2-H_2 in $M(CO)_3(PR_3)_2(\eta^2$-$H_2)$ (M = Tungsten, Molybdenum; R = Cyclohexyl, Isopropyl): Inelastic Neutron Scattering, Theoretical, and Molecular Mechanics Studies. *J. Am. Chem. Soc.* **1990**, *112*, 2324–2332.

(23) Albright, T. A. Rotational Barriers and Conformations in Transition Metal Complexes. *Acc. Chem. Res.* **1982**, *15* (5), 149–155.

(24) Osborn, V. A.; Parker, C. A.; Winter, M. J. Hydride to Carbene Migration at Molybdenum; the Isomerisation of $Mo(H)\{=C[CH_2]_3NMe\}(CO)_2(\eta$-$C_5H_5)$ to $Mo(CO)_2\{\eta^2$-$CH[CH_2]_3NMe\}(\eta$-$C_5H_5)$. *J. Chem. Soc. Chem. Commun.* **1986**, *2* (15), 1185–1186.

(25) Charles P. Casey and Stephen M. Neumann. Reaction of Molecular Hydrogen with Transition Metal Carbene Complexes: Reductive Cleavage of the Carbene Ligand. *J. Am. Chem. Soc.* **1977**, *99* (5), 1651–1652.

(26) Green, J. C.; Green, M. L. H.; Morley, C. P. A Kinetic Study of the 1,2-Hydrogen Shift in a Bis(η-Cyclopentadienyl)Tungsten System. *Organometallics* **1985**, *4* (7), 1302–1305.

(27) Carter, E. A.; Goddard, W. A., III Methylidene Migratory Insertion into a Ruthenium-Hydrogen Bond. *J. Am. Chem. Soc.* **1987**, *109* (2), 579– 580.

(28) Ziegler, T.; Versluis, L.; Tschinke, V. Migratory Aptitude of Hydride and Methyl toward Carbon Monoxide, Thiocarbonyl, and Carbene in $RMn(CO)_4XY$ (XY = CO, CS, CH_2; R = H, CH_3). A Theoretical Study by the Hartree-Fock-Slater Transition-State Method. *J. Am. Chem. Soc.* **1986**, *108* (4), 612–617.

(29) Carter, E. A.; Goddard, W. A. Modeling Fischer—Tropsch Chemistry: The Thermochemistry and Insertion Kinetics of $ClRuH(CH_2)$. *Organometallics* **1988**, *7* (3), 675–686.

(30) Alternative mechanisms in which **Int-1** undergoes CO dissociation to give a pentacoordinated dihydrogen intermediate or in which CO dissociation and H migration occur simultaneously from

Int-2 have been discarded due to their high transition state energy: **TS-2a**, $\Delta G^{\ddagger}_{298K}$ = +42.3 kcal mol^{-1}; **TS-3b**, $\Delta G^{\ddagger}_{298K}$ = +44.0 kcal mol^{-1} (see supporting information).

(31) An alternative plausible mechanism from **Int-5** in which CO dissociation does not take place was calculated to present a similar energy ($\Delta G^{\ddagger}_{298K}$ = +35.9 kcal mol^{-1}) (see supporting information).

(32) The energy span from **4a** to **TS-6** ($\Delta G^{\ddagger}_{298K}$ = +32.8 Kcal mol^{-1}) is similar. These two steps are close in energy and either could be rate-limiting.

(33) Janak, K. E.; Parkin, G. Deuterium and Tritium Equilibrium Isotope Effects for Coordination and Oxidative Addition of Dihydrogen to $[W(CO)_5]$ and for the Interconversion of $W(CO)_5(H_2\text{-}H_2)$ and $W(CO)_5H_2$. *Organometallics* **2003**, *22* (22), 4378–4380.

(34) Bullock, R. M.; Bender, B. R. Isotope Methods – Homogeneous. In *Encyclopedia of Catalysis*; I. Horváth, Ed.; 2000; pp 1–62.

TOC graphic